DEPARTMENT OF DEFENCE
DEFENCE SCIENCE & TECHNOLOGY ORGANISATION
DSTO

Advanced Jindalee Tracker: Enhanced Peak Detector

S.J. Davey, S.B. Colegrove and D. Mudge

DSTO-TR-0765

Advanced Jindalee Tracker: Enhanced Peak Detector

S J Davey, S B Colegrove and D Mudge

Surveillance Systems Division
Electronics and Surveillance Research Laboratory

DSTO-TR-0765

ABSTRACT

This paper presents an analysis of the Jindalee Stage B Peak Detector and highlights a number of deficiencies. Solutions are proposed for these deficiencies and the improvements gained from their implementation are measured. These solutions overcome clustering about the data sample points. In addition, enhancements are made in the areas of: adaptive thresholding to maintain a constant false alarm rate, improved data storage to accommodate non-uniform peak densities, and integration with the adaptive clutter model to associate peaks with the clutter regions.

Published by

DSTO
Electronics and Surveillance Research Laboratory
PO Box 1500
Salisbury South Australia 5108 Australia

Telephone: (08) 8259 5555
Fax: (08) 8259 6567

AR-010-822
June 1999

APPROVED FOR PUBLIC RELEASE

Advanced Jindalee Tracker: Enhanced Peak Detector

Executive Summary

This paper presents an analysis of the Jindalee Stage B Peak Detector and highlights a number of deficiencies. Solutions are proposed for these deficiencies and the improvements gained from their implementation are measured. The result of these improvements is the enhanced peak detector that plays an important role in the advanced tracking system recently installed in the Jindalee Over-the-Horizon Radar.

The primary deficiency of the Stage B Peak Detector is the way that it clusters the detections about the data sampling points. This phenomenon may cause moving targets to exhibit a staircase like progression through the surveillance region. In the radar environment, the automatic tracking system must cope with stationary targets such as transponders. When the detector causes bias it is difficult for the tracking system to discriminate moving and stationary targets. This is particularly the case for slow moving targets. The enhanced peak detector presented in this report is demonstrated to overcome clustering about the data sample points.

The Stage B Peak Detector is also shown to exhibit a high level of error in estimating the location of target detections. This error is apparent from the large scatter of the location of calibration detections. The calibration signal is not propagated by the ionosphere and should display very little positional scatter. The enhanced peak detector presented in this report is shown to dramatically reduce the amount of scatter about the calibration location indicating a more accurate detection process.

The two main developments in the enhanced peak detector to overcome these deficiencies are the use of pre-whitened data and logarithmic compression. The enhanced peak detector detects and locates peaks using the pre-whitened data and only uses the whitened data for signal strength estimation. This reduces the location error and also reduces the incidence of peak splitting that occurred with the Stage B peak detector. The result is a more uniform distribution of noise peaks and reduced bias for target peaks.

The enhanced peak detector also has an adaptive threshold to maintain a constant false alarm rate. This allows the peak detector to use a lower threshold to obtain high sensitivity when clutter conditions are good without swamping the tracker with false detections when clutter conditions are bad. To allow further adaptation to changing clutter conditions, the enhanced peak detector is integrated with an adaptive clutter model. This allows the association of each peak with a clutter zone and associated statistics.

To facilitate these new features and allow for future development, a new data storage approach has been adopted. This gives the enhanced peak detector greater flexibility and creates a simpler interface for the future development of Raid Size and Height estimation algorithms.

The impact of the enhanced peak detector is a higher quality detection process to feed the automatic tracking system. The enhanced peak detector improves the tracker's ability to resolve the ambiguous velocity of radar targets as well as providing more accurate location estimates and smoother region hand-over. By increasing the uniformity of noise detections and associating clutter zone information, the enhanced peak detector helps the automatic tracking system significantly reduce the number of false tracks.

Authors

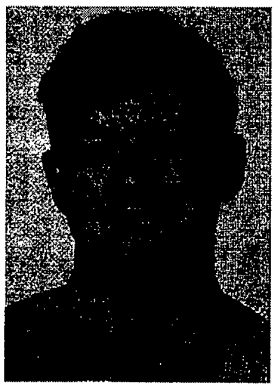

Samuel Davey
Surveillance Systems Division

Samuel Davey completed his BE in Electrical and Electronic Engineering at the University of Adelaide in 1995. In 1998 he completed a Master's Degree in Signal and Information Processing at the University of Adelaide. He has been employed as a Professional Officer at DSTO since 1995 where he has worked in the areas of signal processing and automatic tracking. Samuel's current work involves research into advanced automatic tracking systems and performance assessment of automatic tracking systems.

S B (Bren) Colegrove
Surveillance Systems Division

Bren Colegrove completed his PhD in Electrical Engineering at the University of Queensland in 1973. Since 1973 he has been employed as a Research Scientist by DSTO. Up to 1975 he worked on Microwave Radar clutter modelling. Since then he has worked on Over-the-Horizon Radar. This work involved the design and implementation of the Jindalee Stage B Radar. The initial emphasis of his work was radar system design based on cost minimisation. Subsequent work involved signal processing, displays and automatic tracking systems. From 1979 to 1994 Dr Colegrove was the Australian National Leader of TTCP Technical Panel KTP-2 which concentrates on advancements in automatic tracking systems. Dr Colegrove's present research activities are into advanced automatic tracking systems.

David Mudge

David Mudge was employed as a Professional Officer at DSTO from 1992 until 1995. He worked in the implementation of signal processing and tracking algorithms. David Mudge no longer works for DSTO.

Contents

List of Figures

List of Tables

1. Introduction

Peak detection is used by the Jindalee OTHR signal processing scheme to locate target returns in the azimuth, range and Doppler (ARD) data produced from processing the radar's receiver output. The spatial resolution of an OTHR is quite low (of the order of tens of kilometers) so targets may be treated as point reflectors. It is desirable to locate these point reflectors with sub-cell resolution for the purpose of accurate tracking. Peak detection incorporates interpolation to achieve this improved resolution [1].

The radar data processing is divided into two stages. The first stage takes the time series output from the radar receiver array and forms the time series data from each range and azimuth cell. The second stage forms the frequency spectrum for each range-azimuth cell. The second stage also includes data conditioning algorithms to remove clutter and interference. The final step in stage two involves peak detection where local peaks above a threshold are passed to an automatic tracking system that is part of third stage of processing.

The peak detector used until 1997 was installed in September 1983 with a Probabilistic Data Association Filter (PDAF) for tracking air targets. This system was limited in scope because the Jindalee Stage B OTHR used array processors for all stages of signal processing. Upgrades to the PDAF filter were also limited by the capacity of the array processors.

In 1989, an experimental Joint PDAF tracker was developed in readiness for expected increases in processing capacity. This tracker never performed as well as the Jindalee Stage B PDAF tracker. Some of the reasons were found to be related to the peak detector. Preliminary tests showed that it sometimes formed multiple peaks from a single target return (called peak splitting) and peak locations were biased towards the centre of the radar processing cells.

In 1992 D Mudge conducted research into various methods for removing the bias in the peak detector. His report *Detecting Targets with Sampled Data* was not completed before he left DSTO. S Davey resumed this work in 1996 and this report contains the results on bias reduction by D Mudge with new developments by S Davey.

The report starts with a description of the original peak detector and its defects. The sections that follow give the solution to each defect with an analysis where appropriate. The final sections give additional improvements to the peak detector with the results from tests. In this paper the original peak detector is referred to as either the Stage B or the Jindalee Stage B peak detector. The term 1RSU (Number 1 Radar Surveillance Unit) is used to refer to the current radar system.

2. The Jindalee Stage B Peak Detector.

The PDAF tracking system uses peak detections to initiate and update tracks. The peak detections are found by firstly finding local maxima, referred to as *peak locations*, in the ARD data after data whitening. The ARD data are a three dimensional array of Signal-to-Noise Ratio (SNR) values in units of power for each range, azimuth and Doppler cell. Peak locations in this array are found by comparing each sample point to its immediate neighbours in each of the three dimensions. The sample is declared to be a maximum if the SNR received at that position is greater than each of its neighbours. Referring to Figure 1, the sample labeled *A* is a local maximum if it is greater than all of the points marked *B*.

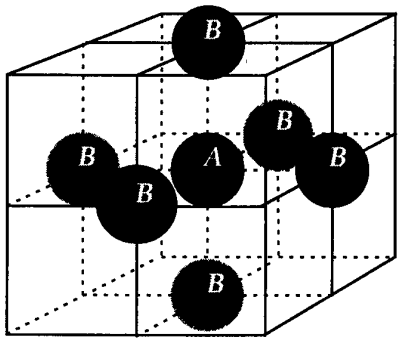

Figure 1 ARD Values Used for Peak Location by the Stage B Peak Detector

This approach to peak location is valid at all data points except for those along the boundary of the ARD data. Here there is no outer neighbour in azimuth and, or range, i.e. no shadow beams and ranges. Therefore the approach illustrated in Figure 1 is modified at the ARD data boundaries to exclude the outer non-existent cell for peak location. In Doppler this problem does not exist as the land clutter is at 0 Hz. Here the peak detector starts and ends 4 cells inside the Doppler cell range that corresponds to doppler frequencies from 0 Hz to Waveform Repetition Frequency (WRF).

In the peak selection algorithm, all of the local maxima for a particular range-azimuth cell are found and sorted by sample SNR value. From these maxima, potential peaks are chosen by selecting the N largest maxima in the range-azimuth cell. Storage for a fixed number of peaks gives a fixed sized array that allows the peaks to be stored according to their location in azimuth-range space. This allows detection and tracking algorithms to efficiently utilise the Jindalee Stage B array processor. However this limit degrades detection performance when there are either multiple targets or a target with spread clutter in a single range-azimuth cell. In a test using a nighttime data set that contained targets, this limit was exceeded in 57 percent of dwells. If we increase the number of peaks in each cell to overcome this limitation, a large percentage of the peak array will be empty. Also there is an increase in the processing time being used to process non-data signals.

Once N maxima have been chosen, the position of each peak is determined by interpolating about the position of the local maximum using a parabolic curve fit, as shown in Figure 2. This reduces the peak detector's measurement error for target tracking. The SNR of each peak is taken from the sample value at the local maximum. After peak interpolation, each peak is compared to a fixed threshold and canceled if it does not exceed it. The thresholded peaks are loaded into the peak array and any unused space is filled with dummy peaks.

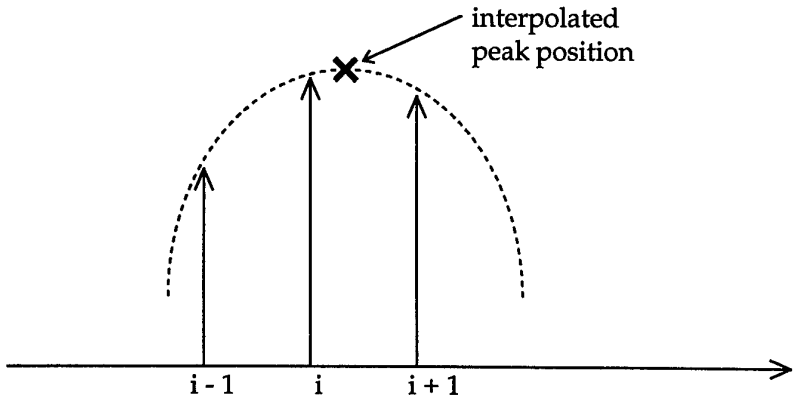

Figure 2 Peak Interpolation Using a Parabolic Fit

As the interpolation process uses neighbours in all directions about a data peak, artificial neighbours are generated for data peaks along the edges of a range-azimuth boundary of the data. The artificial neighbours are formed by using a scaled down value of the edge cell peak value.

The process is summarised in the flow diagram shown in Figure 3.

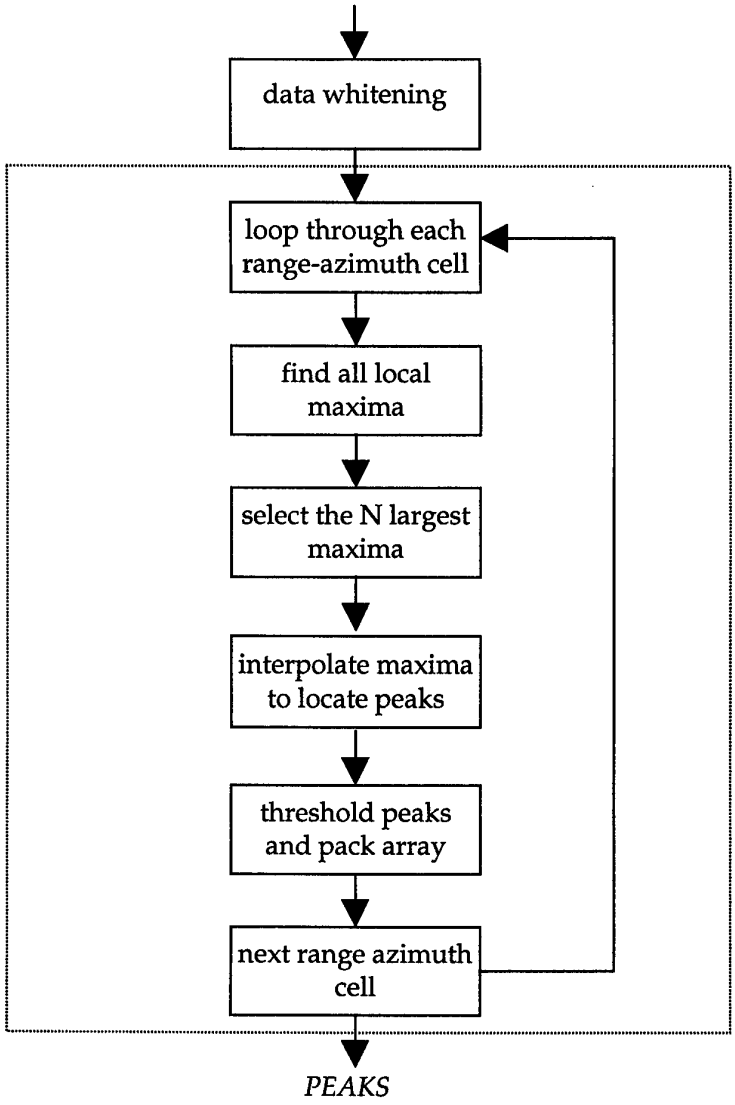

Figure 3 Jindalee Stage B peak detection flow diagram

2.1 Stage B Algorithm Defects

The defects of the Stage B peak detector are best illustrated by the scatter plot in Figure 4. The scatter plot shows the distribution of interpolated peaks in range and azimuth from a single radar region accumulated over 188 radar dwells. The data contains a single target and a stationary calibrate signal. The interference is primarily external. Hence a uniform distribution is expected. Note the tendency for the peaks to be clustered around the range-azimuth cell positions. A similar clustering is found around the Doppler cell positions.

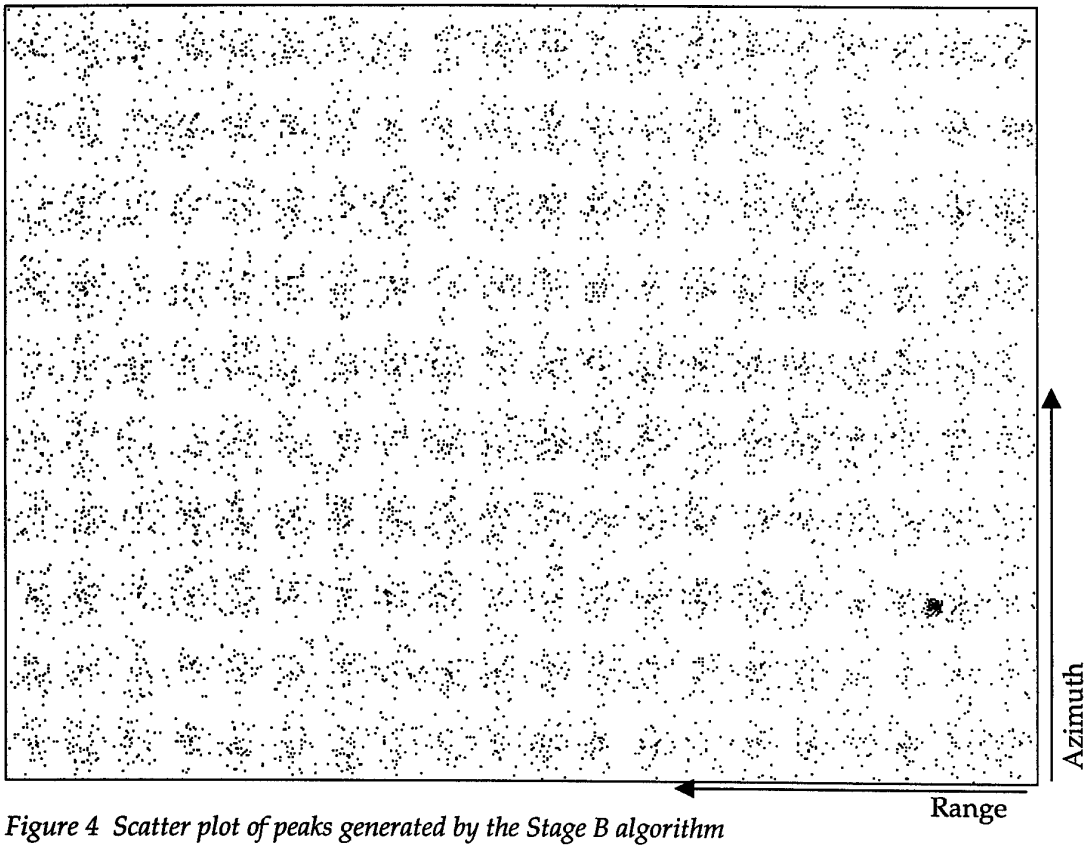

Figure 4 Scatter plot of peaks generated by the Stage B algorithm

The scatter plot highlights the stationary calibrate signal midway between the second and third last cells on the horizontal axis. Instead of there being peaks located at a single point, the peaks are scattered about this position. Analysis of the number of peaks in the region of the calibrate signal did not show any evidence of the peak splitting mentioned in the introduction. Section 4 contains an analysis of peak splitting for a data set containing multi-mode targets.

From the above results and as observed in the introduction, the Stage B peak detector defects are in the areas of :

- Peak interpolation bias errors - including edge effects,
- Peak splitting,
- Inflexible data structures.

The following sections deal with the solution to these problems.

3. Peak Interpolation Bias

The scatter plot in Figure 4 demonstrates the biasing present in the Stage B peak detector. The bias clusters peaks about processing cell positions and makes it more difficult for the tracker to correctly resolve stationary and slow moving targets.

The main causes for this problem are:

Interpolation Function — Errors will occur if the shape of target returns does not closely resemble the parabola used for interpolation. When the target echo is a point source, it is as an impulse in the frequency spectrum. This impulse is then spread by the processing windows in each dimension. Other factors that spread the target returns are non-linear processing steps, additive noise and distortions in the propagation path.

Distortions from Whitening — Peak detection and interpolation is applied to data after the data whitening. Data whitening scales the ARD data to the local noise floor so that whitening data is in SNR. Because whitening is a non-uniform process and because the background noise is non-uniform, it will distort the target return and hence increase the interpolation process error.

A number of other possible causes for the phenomenon were investigated and these are presented in the following subsections.

3.1 Method of Analysing Interpolation Errors and Bias

The original investigation presented the peak detector bias by forming a histogram of interpolated peak locations relative to the processing cells. The histogram uses 100 bins over the range ± 0.5 cell. For interpolation with no bias, the histogram should approximate a uniform distribution. The variance of the observed distribution from a uniform distribution is used as a figure of merit. The variance is normalised for a histogram of 1000 data points. The steps to evaluate the figure of merit are shown in Figure 5. Here M represents the actual number of data points used for the histogram and N is the number of bins.

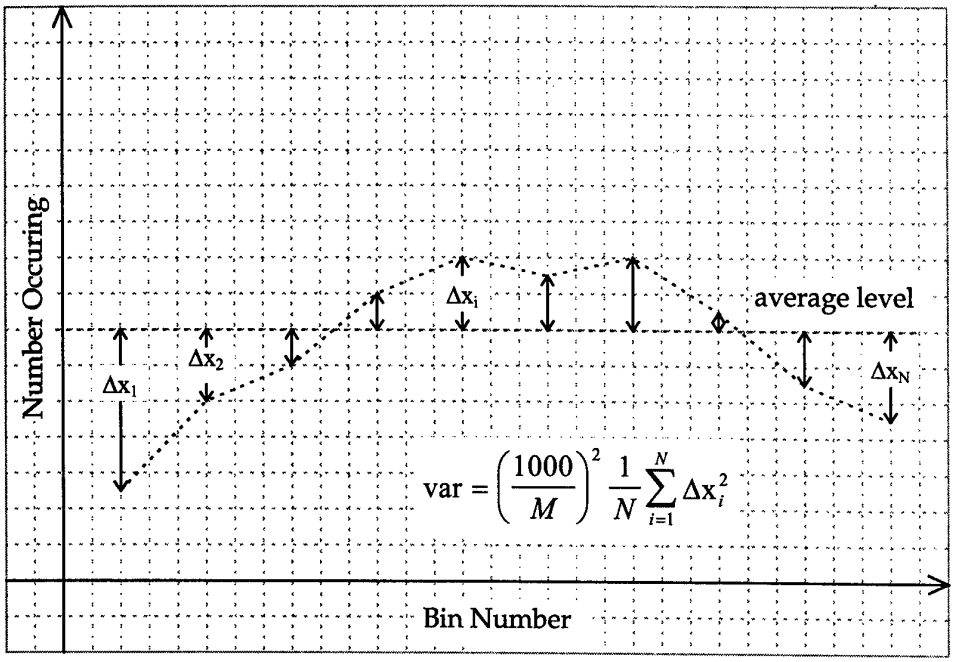

Figure 5 Normalised variance calculation

3.2 Bias Correction by Data Compression

Because a parabola gives a simple interpolation algorithm, the approach taken to investigate the centering was to alter the data values so that the shape of returns gives a better match to a parabola. The best results came from compressing the data. This action maintains the peak location. The compression techniques investigated were:

a) Square root the data array values before interpolation. Because this reduced the bias, tests were also made with 4th and 8th roots.

b) Conversion of the data values to decibels (i.e. SNR values) before interpolation.

Data compression was tested on both simulated data and actual OTHR data. The results set out in Table 1 and Table 2 show the histogram variances for each case respectively. It can be seen that both the 8th root and the decibel techniques provide significant improvement in performance. The best performance for OTHR data is achieved with the decibel technique.

	8th root	4th root	Square root	dB	Baseline
Azimuth	1091	1170	1298	916	2104
Doppler	999	989	998	965	1269
Range	927	967	1228	883	1562

Table 1 Histogram error variances for data compression of simulated data

	8th root	4th root	Square root	dB	Baseline
Azimuth	2270	2668	3467	1987	5256
Doppler	229	279	401	189	719
Range	956	1153	1625	770	2744

Table 2 Histogram error variances for data compression of OTHR data

While the 8th root and decibel techniques provide similar results, the 8th root technique is much slower. This is due to the implementation of exponents by compilers. The algorithm for taking the nth root of a number is shown below.

$$y = \exp\left(-n \times \log(x)\right) \quad \equiv \quad y = \sqrt[n]{x}$$

The algorithm contains an exponential operation and a logarithm both of which are quite computationally expensive. The exponential and logarithm are approximately the same speed for operation and so the decibel technique takes approximately half the time of the 8th root. This makes the decibel technique much more desirable.

3.3 Bias Correction by Look-up Table

Another method for correcting the bias is to use a look-up table to adjust for systematic errors in the interpolation process. The interpolation error is a function of SNR with the largest errors at low SNR. To test the viability of the look-up table method, the table values were chosen to correct the interpolated position of a 100dB target.

	Look-Up	Look-Up on 8th Root Data	Look-Up on dB Data	Baseline
Azimuth	1979	2494	2599	5256
Doppler	176	207	223	719
Range	925	1114	1154	2744

Table 3 Histogram variances for look-up correction of OTHR data

Table 3 gives the variances using corrections from a look-up table. The performance is similar to data compression using the log function. Also listed in Table 3 are the variances when data compression with the 8th root and log functions is used in conjunction with a table look-up. For this case there is a slight degradation in performance.

The look-up table method requires fewer operations than data compression because it only involves a table interpolation and subtraction per interpolation dimension. Improvement in performance is expected by adding SNR to the table but this also adds more operations. One feature of the look-up table approach is the need to have tables

for each significant change in signal processing weights. A related issue is the unknown sensitivity of the look-up table to signal distortions introduced by the ionospheric medium. Because of these issues and because the simplified implementation gave similar performance to data compression with a log function, the look-up table is not developed any further.

3.4 Bias Introduced by Peak Thresholding

The Stage B peak detector applies thresholding to the data value at the sample point, i.e. the radar processing cells. Consider a target peak with an SNR value just above the detection threshold. If the position of the signal maximum is midway between two sample points, the sample values will be lower than the threshold. Alternatively, if the maximum is close to a sample point, the sample will exceed the threshold. This effect is sometimes called scalloping loss. Hence signals just above the threshold and occurring near the sample points are more likely to be passed by the peak detection routine than similar signals near the midpoint between samples. This is illustrated in Figure 6. The left return will give a peak, but the right one will not.

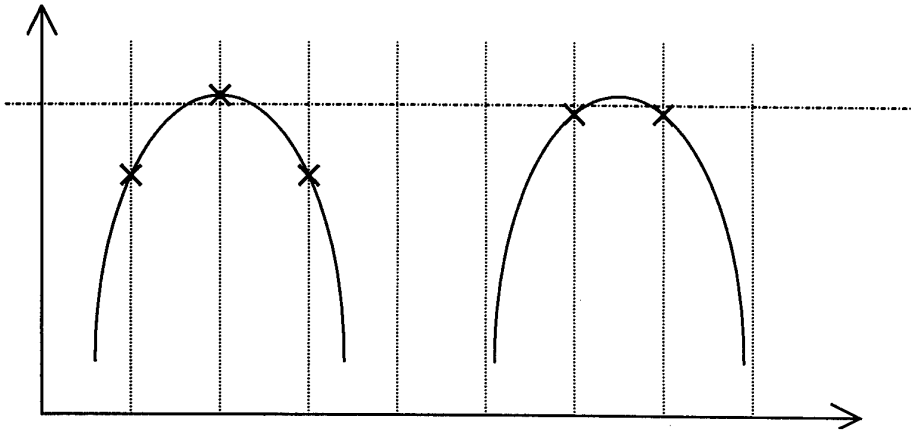

Figure 6 Rejected returns due to sample positioning

The way to remove this possibility is to interpolate in SNR before applying the threshold for accepting peaks. Interpolation has the added advantage of removing SNR fluctuations introduced as the target moves between the radar processing cells.

SNR interpolation is added by calculating the maximum of the parabola fitted to the sample point and its neighbours. The threshold can then be applied to the interpolated peak value. In this way, the same thresholding criteria is applied to all peaks irrespective of their position relative to the sampling points, and a more even distribution should result for signals near the detection threshold.

3.4.1 Multidimensional Interpolation

We need to extend the above process of interpolation for quadratics of a single variable. We want to interpolate the amplitude as a function of three variables: range, azimuth and doppler shift. It is fairly simple to do this if we model the target return as shown in equation (1).

$$A(r,a,d) = F(r) \times G(a) \times H(d) \tag{1}$$

That is, we assume that the amplitude function of the target return is separable. With the model in this form, we can find the peak in each dimension independently (this is the process used for position interpolation). We may calculate the value of the maximum (the interpolated peak) using equation (2).

$$A(r_m,a_m,d_m) = A(r_0,a_0,d_0) \times \left\{ \frac{F(r_m)}{F(r_0)} \times \frac{G(a_m)}{G(a_0)} \times \frac{H(d_m)}{H(d_0)} \right\} \tag{2}$$

where (r_m, a_m, d_m) are the coordinates of the maximum and (r_0, a_0, d_0) are the coordinates of the ARD data peak. The expression in brackets is a correction factor applied to the sample value to obtain the local maximum. We assume that it is valid to approximate the unknown functions F, G, H near the sample maximum using parabolic interpolation.

Each of the ratios to the right of equation (2) are calculated separately. The first ratio, $F(r_m)/F(r_0)$ is written as

$$\frac{F(r_m)}{F(r_0)} = \frac{F(r_m) \times G(a_0) \times H(d_0)}{F(r_0) \times G(a_0) \times H(d_0)} = \frac{A(r_m,a_0,d_0)}{A(r_0,a_0,d_0)} \tag{3}$$

where the term $A(r_m, a_0, d_0)$ is the peak value obtained by applying one dimensional parabolic interpolation in range. Similar expressions are used for the azimuth and doppler ratios in equation (2). The ratios are then substituted into equation (2) to obtain the interpolated peak value.

$$A(r_m,a_m,d_m) = \frac{A(r_m,a_0,d_0) \times A(r_0,a_m,d_0) \times A(r_0,a_0,d_m)}{A(r_0,a_0,d_0)^2} \tag{4}$$

Note that the form of the interpolation equation is the product of one dimensional interpolations. This is due to our initial assumption that the target return provides a separable function.

3.4.2 Effect of Amplitude Interpolation

The amplitude interpolation technique was included with the Stage B peak detector and the effect that it had on recorded OTHR data was tested. There was a significant rise (17%) in the number of peaks with a fixed threshold. However, the additional peaks were still clustered about the sample points. Only a small improvement in the distribution was observed. This is illustrated by the variances calculated from recorded data in Table 6.

	Interpolated	Baseline
Azimuth	4452	5256
Doppler	520	719
Range	2159	2744

Table 4 Histogram variances for amplitude interpolation on OTHR data.

The process of interpolating the peak SNR moves the peak probability density function. It increases the mean and modifies the variance of the distribution. The distribution of interpolation corrections is approximately a gamma distribution as shown below in Figure 7.

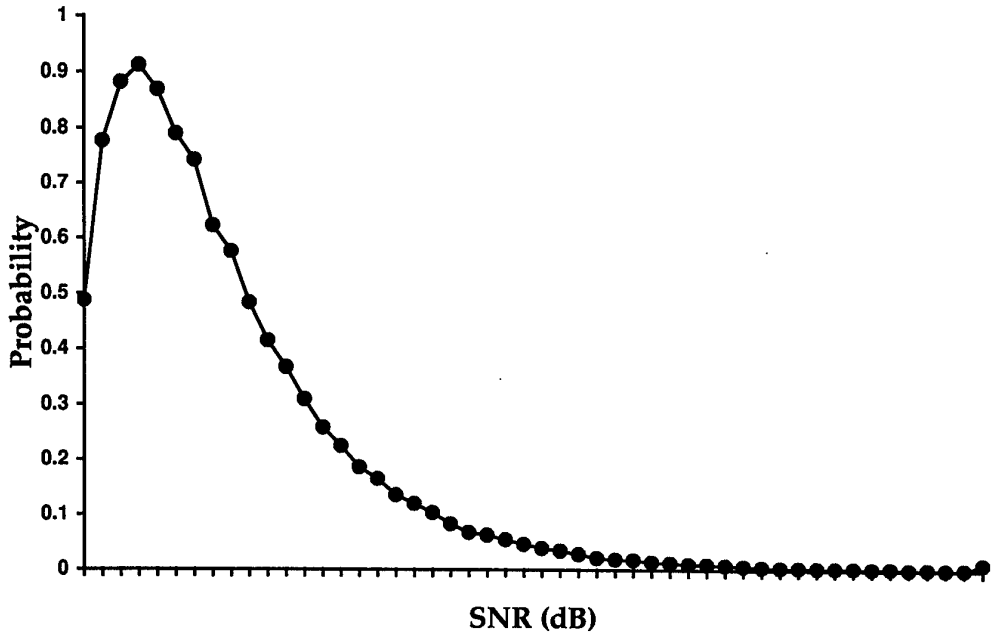

Figure 7 Interpolation Correction Distribution

3.4.3 Implementing a Dynamic Peak Threshold

Amplitude interpolation, the number of targets and OTHR clutter variations change the number of peaks above a fixed threshold. To achieve a constant false alarm rate, a dynamic threshold is applied to the peaks. The method chosen to implement the dynamic threshold involves forming a cumulative distribution function of the peak SNR values. This distribution has a resolution of say 0.5 dB and the threshold is chosen by selecting the SNR with the required number of peaks.

The cumulative distribution requires a separate array of peaks (that will not be used in data output) with all of the unthresholded peaks in the dwell. As a peak is found, the cumulative distribution array is updated. This array is indexed by SNR and each element contains the number of peaks with an SNR greater than the SNR corresponding to the index value. For example, we might form a distribution with thirty entries in steps of 0.5 dB. A fabricated distribution of this form is shown in Table 5. If we are choosing say 200 peaks for each dwell, the threshold in this case would be chosen to be 6.0 dB.

SNR value	number occurring
0	453
0.5	387
1.0	344
5.5	225
6.0	198
6.5	162

Table 5 Example Peak Distribution

To successfully implement a dynamic threshold, we cannot use a peak array data structure that has a fixed number of peaks per range-azimuth cell. A new data structure for use with a dynamic threshold is described in Section 5.

3.5 Bias from Peak Interpolation on the ARD data boundary

The artificial neighbours generated for non-existent data points along the range-azimuth boundary of the data introduce a peak interpolation bias. This increases the measurement error of target peaks by adding a bias that causes tracks to kink as they cross-region boundaries.

Also, because the peak detection process uses fewer neighbouring points to locate a peak, ie 5 instead of 6, the edge cells have a higher number of peaks. This contributes to an increase in the number of false tracks along the region boundaries.

The correction of this problem involves the addition of shadow beams and ranges to the stage one and two processing. The peak detector is then able to use the same peak location and interpolation algorithm over all ARD cells.

3.6 Bias from Sub-Array Beam Pattern

The receiving array beamforming is performed in two steps. The first consists of multiple delay line beamformers that are connected to form overlapped subarrays. The output from the subarray beamformers is input to the radar receivers which contain A/D converters. The binary data is then used as input for the final step of the beamforming process that forms the simultaneous fingerbeams. Figure 8 illustrates the subarray beam (dashed line) and the 6 central fingerbeams with 2 shadow beams. This figure also shows the sidelobes formed by this two step beamforming process.

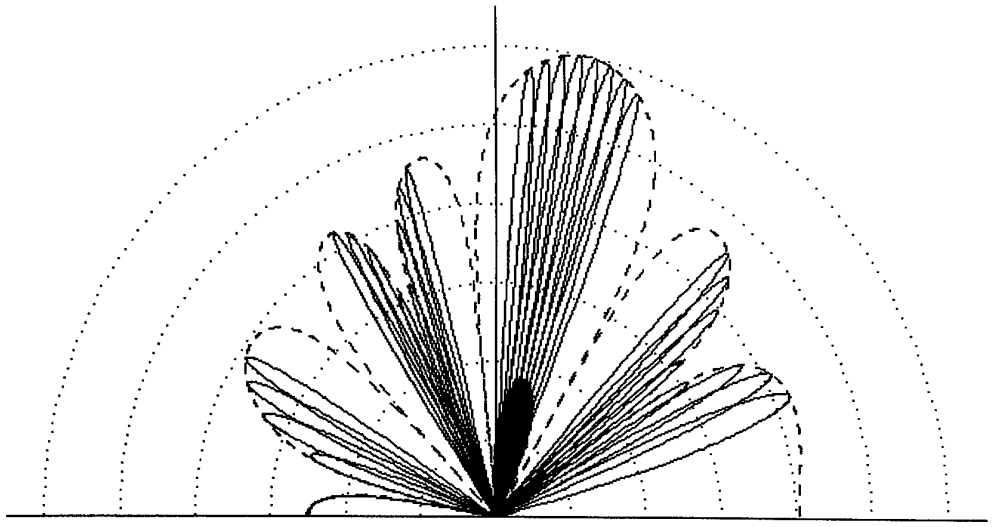

Figure 8 Subarray antenna pattern

The main feature of Figure 8 that contributes to a bias in the interpolation is the tapering of the fingerbeam gain. This leads to an azimuth bias towards the central fingerbeam. The method for correcting this bias is found from the radar equation. For the case of an externally noise limited system with a target at a fixed location, the radar equation gives the SNR proportional to the following system parameters.

$$SNR \propto \frac{P_t G_t g_r}{N_0}$$

Where P_t is the transmitter power, G_t is the transmitter gain, g_t is the receiving array gain and N_0 is the noise power spectral density. For a particular target, only the receiving array gain varies because of the fingerbeam overlap - the transmitting power and gain serve only as a target illuminator. So the transmitting array beam shape does not contribute to any bias in target location, it only alters the maximum target SNR. Also the noise power does not depend on antenna gain. Therefore the only correction required for the change in gain is that from the subarray beam shading.

This correction applies to the peak selection and interpolation. Note that correcting for the antenna gain alters the peak location in azimuth. The correction is applied by scaling the pre-whitening data using a fixed array. The values in this array are determined by the sub array shading and are almost constant as the steer direction is changed. The whole of the pre-whitening data array is scaled before peak detection.

3.7 Recommendations for Correction of Interpolation Bias

From the above analysis, reduction of the interpolation bias errors in the Stage B peak detector requires the introduction of the following changes.

a) Data compression with a log function to give SNR in dB.

b) Amplitude interpolation. (Note that amplitude interpolation does not significantly reduce bias, but it does improve the accuracy in the measured SNR.)

c) Addition of shadow beams and ranges to ARD data.

d) Correction for the fingerbeam gain taper by the subarray. (Note that this change does not contribute to the bias observed in noise peaks because the noise is isotropic. However, it adds an error to the interpolated azimuthal position for true target returns.)

With these changes implemented, the new variances for tests performed on OTHR data are given below in Table 6. The relative improvements are different for each dimension. This is probably due to the fact that different windows are applied for each dimension in the signal processing.

	Proposed improvements	baseline
Azimuth	1021	5256
Doppler	54	719
Range	228	2744

Table 6 Histogram variances with recommended improvements implemented

4. Peak Splitting

The tendency of the Stage B peak detector to produce multiple peaks about a single target return is particularly evident for high SNR returns. The Jindalee PDAF tracking filter assumes that a target gives a single return. The new multiple model track initiation filter [2] is particularly sensitive to multiple closely spaced peaks because they can make velocity ambiguity resolution more difficult.

One cause for the splitting effect is skewness of peaks in the ARD data. A mild skew exists because of the range-Doppler coupling that is introduced by processing the waveform in two stages, i.e. range followed by Doppler processing. Also skew can be introduced by noise. Figure 9 demonstrates how skewed data gives extra peak detections. Point *A* is the true peak, however, points *B* and *C* will be declared as peaks because of their neighbours. The neighbours used for maxima definition are shown as unfilled circles.

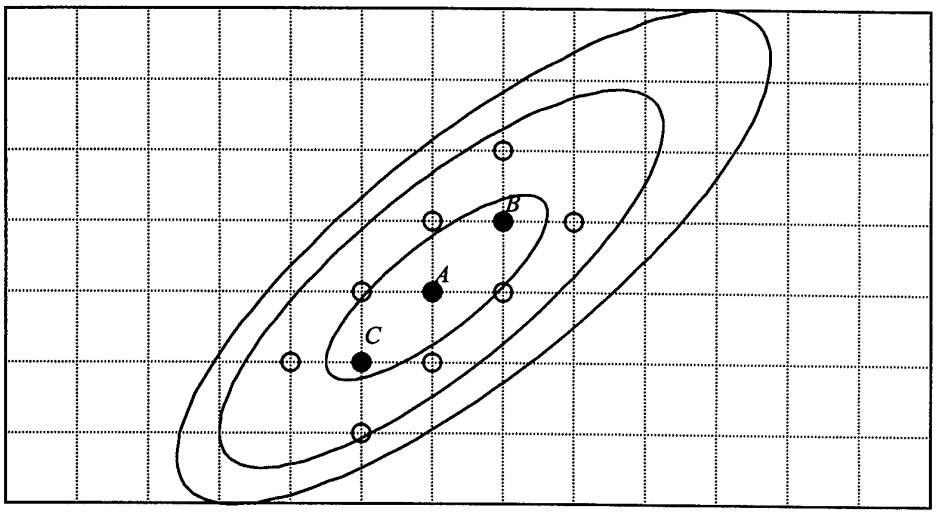

Figure 9 Peaks formed by skewed ARD target returns

Another cause for splitting is a result of the peak selection being after the data whitening process. The Stage B whitener scales the ARD data by dividing it into Doppler bands followed by range bands. In each band a trimmed mean is calculated for scaling the data. Thus the whitener scales the data in each band by a slightly different level, which can lead to a single broad peak being split into a cluster of peaks as shown in the one dimensional example in Figure 10. A similar splitting of peaks may arise from multiple-mode propagation. In this case the target returns from different propagation paths are displaced in Doppler as well as range. The multi-mode returns may bias the whitener leading to distortions in the shape of the peak which will give clustering as well as interpolation errors.

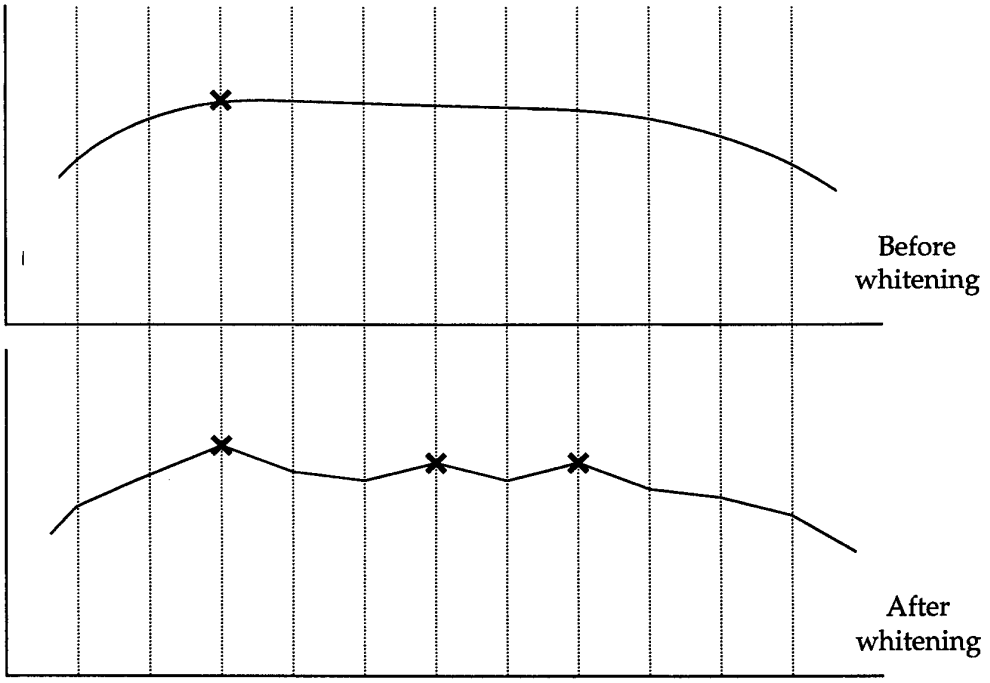

Figure 10 Whitener Effect on Broad Peaks

The solution to this defect involves altering the method of peak selection and its relation to the whitening process. One approach investigated increased the power of each sample by a weighted sum of its neighbours. The weights were based on the ARD processing windows. After performing the weighted sum for all ARD cells, the previous peak selection criterion was used except that in this case the power array was used instead of the data array. This approach would tend to have a smoothing effect and reduce the occurance of peak splitting. The performance was sensitive to the values in the array of weights and in some cases the peaks were not in the correct location. So this approach was not pursued any further.

The solutions given in the following sections do not alter the ARD data values but deal with alterations to the peak selection procedure and its point of application in the processing sequence.

4.1 Peak Location with all Neighbours

To stop skewed peaks in the ARD data forming multiple peaks, the sample neighbourhood is extended to include cells on the diagonal as shown in Figure 11. These extra cells increase the number of cells tested for peak selection from 7 to 27. This prevents the formation of multiple peaks as shown in Figure 9.

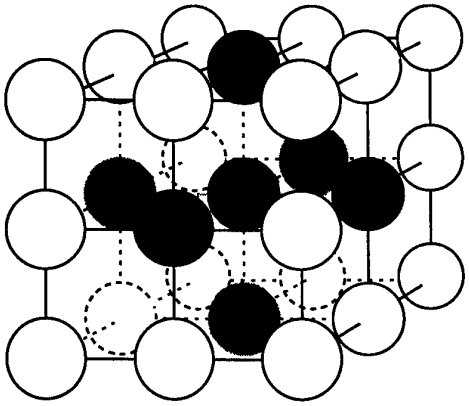

Figure 11 Modified neighbourhood for local maxima

The peaks produced using the modified neighbourhood have been compared with those using the standard six neighbour system. The comparison used the same data set that produced the scatter plot in Figure 4. This data contains a single target propagated via a single mode. In this case the number of peaks per dwell was counted for both methods of peak location with a fixed threshold. Figure 12 shows the percentage reduction in the total number of peaks per dwell as a function of time. On average, the number of peaks is reduced by at least 15 percent. This is clear evidence of a reduction in splitting.

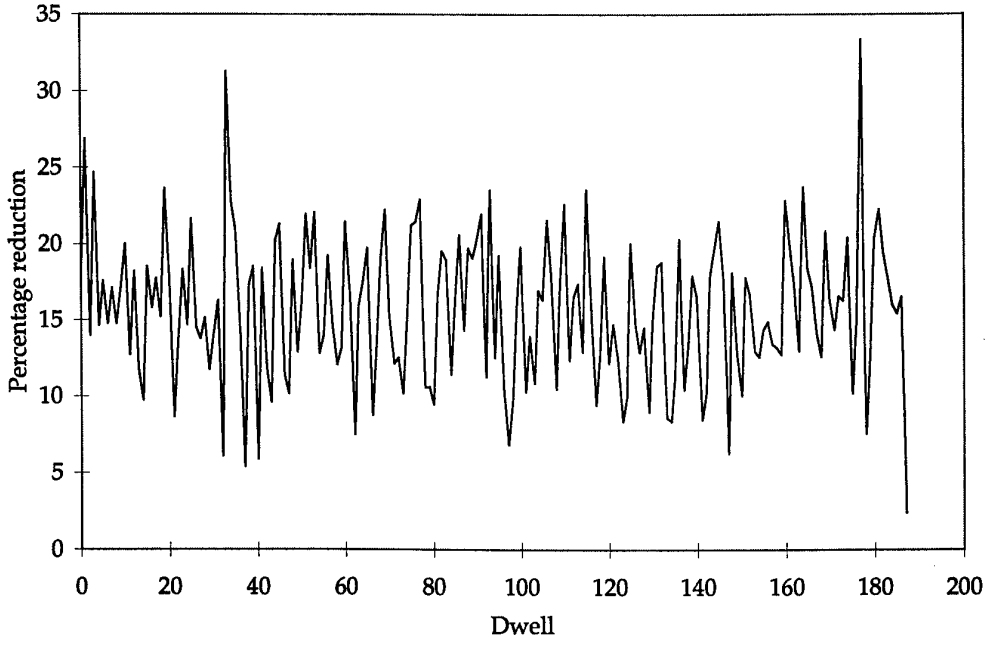

Figure 12 Reduced number of peaks from using all neighbours

4.2 Peak Detection on Pre-Whitening Data

As noted previously, it is highly desirable to use data before the whitening process for peak location and interpolation. This involves saving the pre-whitening data for later use by the peak detector. The tracking system has been found to work best with the SNR of peaks rather than the absolute power. For this reason peak SNR is retained.

The data prior to the whitening process is not in a form that is suitable for determining the SNR of peaks because the background noise is not white. It is possible to convert the data to an absolute scale (such as dBm) but the thresholding for peak selection would need to vary with conditions (particularly range). Instead the data is normalised by using the same value to scale every point to get an average noise floor of unity. Because the data may not be spatially uniform, the sample levels derived at this point will not give a true measure of the peak SNR. The SNR must be derived from an approximation to the *local* noise level. This is what is performed in data whitening.

This means that we need the whitening data to obtain peak SNR values and the pre-whitening data to locate and interpolate maxima. This leads to the flow diagram shown in Figure 13.

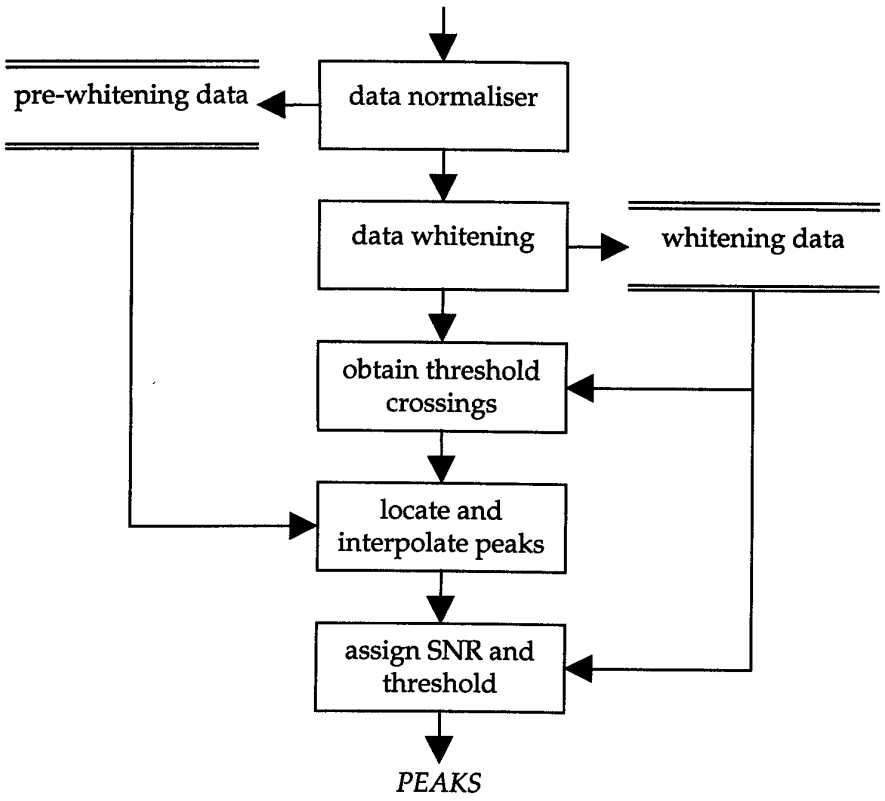

Figure 13 Data Flow Diagram of peak detection on pre-whitening data

In Figure 13 the "locate and interpolate peaks" uses the pre-whitening data to search for peaks in the area defined by the threshold crossings. This is more computationally efficient than searching all of the pre-whitening data for peaks and then removing those peaks that did not pass the threshold test. Here the peak location uses the all neighbour approach in section 4.1. The final process to "assign SNR and threshold" to the peaks uses the algorithms outlined in section 3.4.

The algorithm based on Figure 13 was quantitatively examined by observing the number of peaks over 15 dB found in a data set. This level is well above the noise and we would expect any peaks found to be caused by target signals. The number of peaks was counted for the pre-whitening method and for the standard post-whitening method. The difference between the two (post-whitening method subtract pre-whitening method) is plotted in Figure 14 below. Positive numbers indicate that the pre-whitening method found less peaks than the post-whitening method. The data used for this analysis was from a single radar region over Darwin airport. The region contained several targets as well as the Darwin beacon. Propagation was present in two ionospheric layers so there were three propagation modes for each target. This produced a large number of signals above 15 dB.

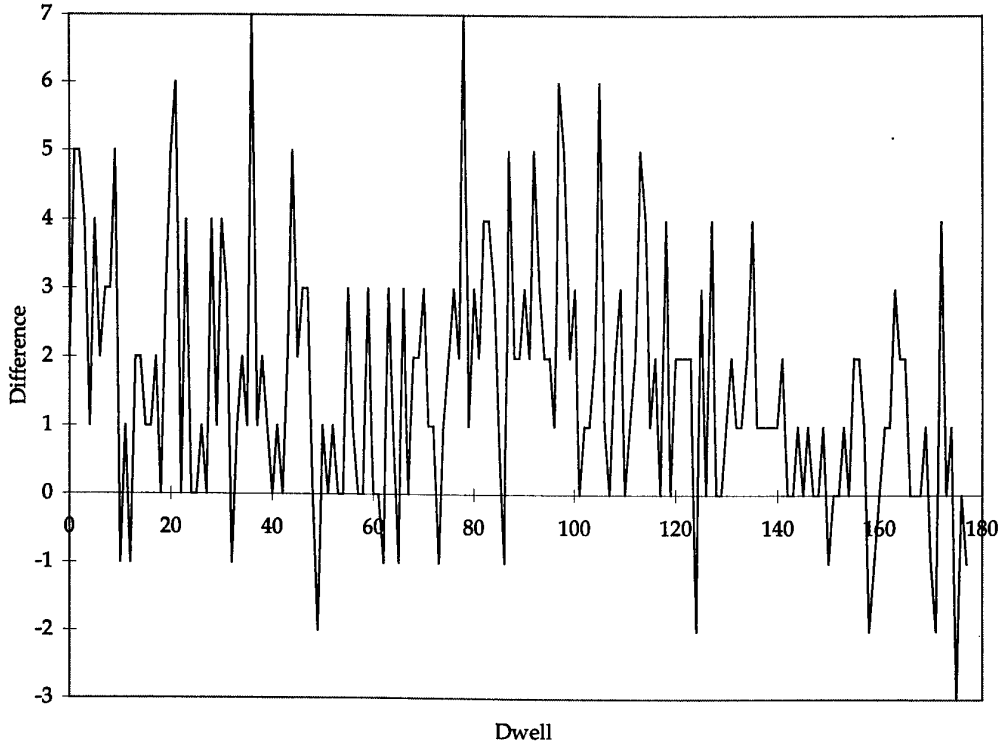

Figure 14 Improvement by peak detection on pre-whitening data

As can be seen from Figure 14, the pre-whitening method reduces the number of multiple peaks on average. One unexpected result was that the pre-whitening method gave more peaks in about 10% of cases. These were not investigated because of the low number but the results show that the whitener occasionally smoothes the data, thereby suppressing peaks.

5. Peak Data Structures

The final issue addressed is the modification of the peak detection scheme to use data structures that incorporate greater flexibility. The current peak detection scheme uses fixed array dimensions to store all of the details about each peak. This structure is simple and suitable for an array processor that does not have dynamic data storage. The array is made reasonably large to cope with areas of high peak density and has space allocated for N peaks in each range-azimuth cell. Overall, the number of peaks found in a dwell of data is commonly around one hundred. This is about one eighth of the space allocated in the array.

The Stage B tracker assumes an *a priori* distribution for false alarms with a preset detection threshold for peaks. The Stage B peak detection scheme described in Section 2 has an unknown higher detection threshold when the number of peaks per range-azimuth cell exceeds the upper limit. If the upper limit for the number of peaks stored is N and the number of peaks found is M, the above situation arises when $M > N$. In this case we have $(M - N)$ peaks above the threshold that are discarded. This is equivalent to increasing the threshold by an unknown amount for the range-azimuth cell that has the M peaks.

This effect can be beneficial when a large number of peaks are formed due to meteor activity or spread clutter as the number of false peaks in the area is limited. This prevents these areas from capturing an excessive number of peaks at the expense of areas with less clutter. However, it does invalidate the tracker's *a priori* threshold assumption.

Since array processors are no longer used for 1RSU, the fixed data structures are replaced by a scheme that has a fixed upper size for the number of peaks in each dwell. This allows a reduction in the amount of data transmitted between machines.

The fixed upper limit is achieved by adapting the detection threshold to keep a near constant number of peaks in each dwell with a variable number of peaks per range-azimuth cell. This leads to a known threshold that is uniformly applied across the whitening ARD data. This system also allows the implementation of other thresholding techniques such as a higher threshold in cluttered areas. What is important is that the tracker now has accurate knowledge of the threshold for probability calculations under all conditions.

To remove the problems described above it is necessary to allow the number of peaks stored in a particular range azimuth cell to be dynamically altered. Therefore, the data structure used for peak storage needs to be more adaptive. We will now consider possible new data structures.

5.1 Linked Lists

We could optimise the space used in peak storage by using a linked list of peaks (see appendix A). In this case we would be allocating only enough space as was required by the peaks that were found. We would not need to limit the number of peaks to any maximum value because we would be using dynamic memory allocation.

5.1.1 Shortcomings with Linked List Approach

The linked list approach is not appropriate for use within the 1RSU signal processing structure for several reasons. The first reason is an incompatibility with Fortran. Fortran is the language used for the peak detector code. Fortran does not have suitable pointer structures and dynamic memory allocation. This is not a major problem since we can write the list functions in a more suitable language such as C and call the functions from the peak detection code, however, it adds to the overall completity of the software.

A more serious problem is that a list structure requires a set of pointers into the list to identify which peaks belong to particular range azimuth cells. The tracker requires these pointers for the association of peaks to tracks. This requirement is best achieved by creating an array of lists rather than a single list.

The third problem, however, is more fundamental. Linked lists are pointer based structures and as such, the only data stored in the array would be pointers to memory locations where the peaks are stored. In the 1RSU signal processing suite, the stage2 and stage3 processes run on different machines. This means that if we passed the linked list and pointers from stage2 to stage3, the receiving task would locate this data in different memory locations in the stage3 processor. Hence the pointers would be pointing to the wrong memory locations in the stage3 processor. To avoid such problems, we would need to "undo" the linked list by packing all the peaks together and then sending this array to stage3. In stage3 we would need to reconfigure the linked list and pointers. This is all a bit pointless as we could just use the packed array for all steps.

These difficulties are a feature of the pointer nature of the structure and so all other pointer structures (such as trees) will be faced with them.

5.2 Packed Array Structure

One way that we can implement a list structure without using pointers is to use a fixed size array. Each new data point is entered into the array after the last. We do not need pointers to following data entries because we can find the next entry by incrementing an array index. This structure has a few shortcomings also.

When compared with a linked list, deletion of data from the array becomes a very computationally intensive procedure. If data is deleted from the middle of the array, then the end of the array must be shuffled along to fill the space. This is required to maintain the correct ordering of the list elements. In a linked list it would be a simple matter of reallocating one pointer. Similarly, adding new data to the middle of the list becomes difficult (the same shuffling is required).

Because we are not using the array as a true data-base we can ignore the problems above. Data will never need to be deleted from the array (peaks are currently *canceled* by giving them cancel values). If we process the data in a meaningful order and always add peaks to the end of the list, the peaks will be stored in that same order. To allow for a variable threshold, a temporary working array is used. Once a

suitable threshold has been decided, the peaks above this threshold are moved into the output peak array.

5.2.1 Indexing the array

Like the linked list structure, the list array needs some additional information to allow us to identify peaks in some given area. This is done by creating an array of peak indices. In the stage3 processing, the tracker requires to access peaks based on the range-azimuth cell in which they are detected. To enable efficient access to the peaks the peak indices array stores an index into the peak list array where the first peak for a particular range-azimuth cell is stored. The array also stores the number of peaks found in each range-azimuth cell. If no peaks are found in a particular cell, both of these fields are set to zero. Combining these two structures, we now have the capability of applying a variable threshold to the whole dwell whilst not limiting the number of peaks in any part of the dwell.

The peak list array and the peak index array are show below in Figure 15.

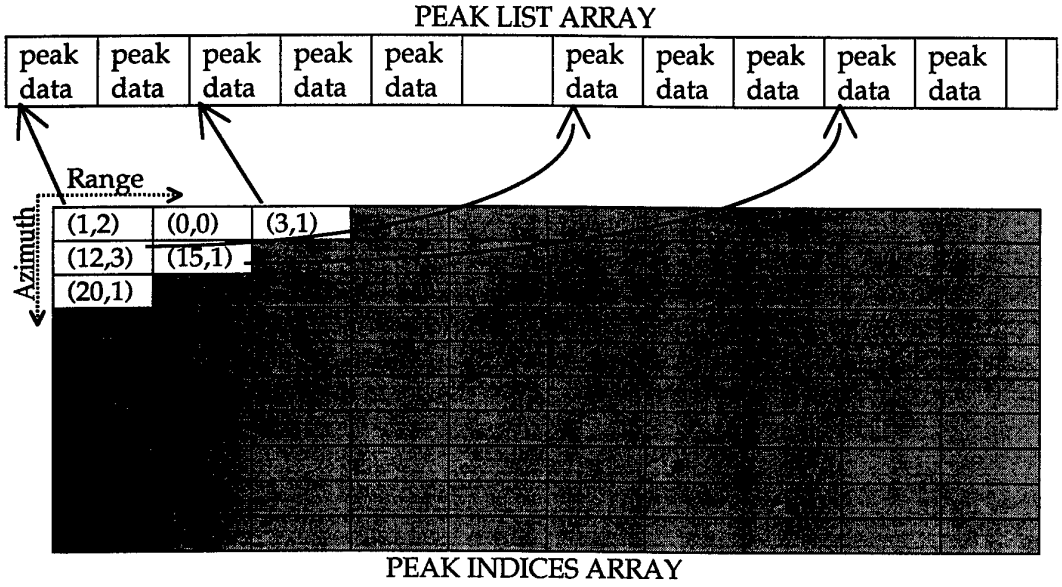

Figure 15 Peak detection data structures

Each of the entries in the peak list array contains information about a peak. This information is the position of the peak in azimuth, range and Doppler and also additional characteristics such as peak SNR.

6. Implemented Peak Detection Improvements

The changes detailed in the previous sections have been brought together to produce the enhanced peak detector. The enhanced peak detector has also been integrated with the adaptive clutter model developed by Branko Ristic [3]. This clutter model develops a map in azimuth-range-doppler space that divides each data set into clutter zones. The probability density functions for those zones are recursively estimated using histograms of the peaks found in each clutter zone. Part of this process is performed during peak detection and part of it is performed by the tracker.

When a new dwell of data arrives, the first step is to form the clutter map. This is a multidimensional array that classifies every point in azimuth-range-doppler space as one of a number of clutter zones. This mapping procedure uses the whitening array as a starting point and uses various image processing techniques to produce the clutter map [3].

Once the clutter map is formed, peak detection is carried out and the map is used to associate every peak found with one of the clutter zones. Relevent clutter zone statistics such as zone ARD volume and the total number of peaks in each zone are calculted. The map statistics (not the map itself) are then passed on with the peak data and the tracker performs the remaining parts of the clutter modeling. Namely the recursive formation of clutter zone probability density functions based on the distribution of peaks in each zone.

The peak detector also uses the surface clutter edges formed by the data whitener as boundaries for detection. In the whitening process, the Ordered Statistic Whitener identifies the edges of the surface clutter for each range azimuth cell using the clutter suppression algorithm. This can give a different maximum and minimum clutter edge for each range azimuth cell. These clutter edges are used to prevent the peak detector from looking for peaks in the surface clutter. Because this has an impact on the peak distribution in doppler space, the clutter edges calculated are stored in the peak index array.

The changes described in the previous section result in a very different method for peak detection. The modified algorithm based on the flow diagram in Figure 13 is described below and an expanded flow diagram is shown in Figure 16.

The new method for peak detection is as follows:

1. Form the clutter map using the array of whitening factors for each sample point.
2. Using the whitening data array, locate positions where the whitening data passes above a minimum threshold.
3. At each of these threshold crossings determine if that cell corresponds to a local maximum in the pre-whitening data.
4. For each local maximum use the pre-whitening data to interpolate the peak in position and determine the SNR using the whitening data.

5. Save each interpolated maximum into a temporary peak array and update a cumulative distribution of the SNRs of local maxima for this dwell.
6. Determine the threshold required to obtain a desirable number of peaks for tracking and save this value for later use.
7. For each maximum that crosses this threshold, save the interpolated peak parameters and the associated clutter zone in the peaks array.
8. Update the array of indices into the peaks array for use by tracking

As shown in Figure 16, the data passed to the tracking system are: peak index array, peak list array, SNR threshold, and the clutter map statistics.

Pseudo code for the algorithm is set out below.

```
For each beam
    For each range
            For each doppler
                    If whitening data cell is above minimum threshold
                            If pre-whitening data cell is a local maximum
                                    Interpolate peak using pre-whitening data
                                    Store peak data in potential peaks
                                    update distribution table
            endfor {doppler}
    endfor {range}
endfor {beam}

Using distribution table, select threshold such that the total number of peaks ≤ N

For each peak in potential peaks
    If peak SNR is above threshold
            Store peak data in peaks array
            Update peak_indices
endfor {peak}
```

The algorithm flow diagram is illustrated below:

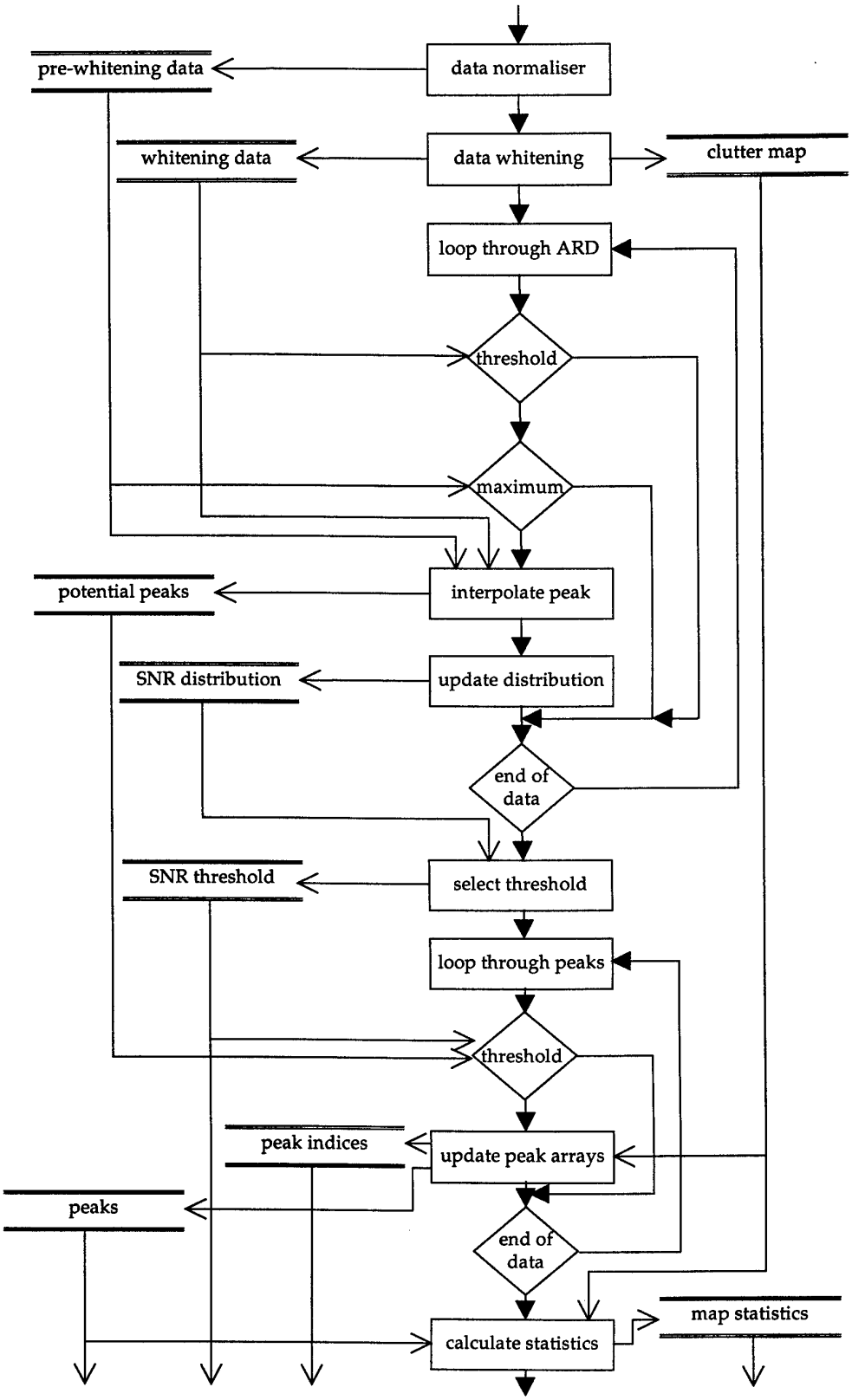

Figure 16 Modified peak detection flow diagram

7. Test Results

We will now undertake a comparison of the performance of the two peak detection algorithms. Firstly, let us consider the peak location accuracy.

7.1 Peak Location Accuracy

It is difficult to measure the accuracy of the peak interpolation procedure with experimental data because we do not know where the target peaks truly lie. However, for this analysis, we have used the artificially injected calibration signal in the 1RSU system. This signal is injected in the middle of Doppler space at a fixed position in range and azimuth for each dwell. It is actually injected in between the cell sample points. We have therefore taken a scatter plot of the peaks generated near the injected position of the calibration signal. The plot was constructed using the peaks declared over the space of 188 different dwells of clean noise data. That is, the data was not corrupted by meteors, lightning, spread clutter or radio frequency interference.

The scatter plots for the two algorithms are shown in Figure 17. They show all of the peaks found near the injected calibration signal and are plotted as range against azimuth. The Stage B peak detector is shown on the left and the modified peak detector on the right.

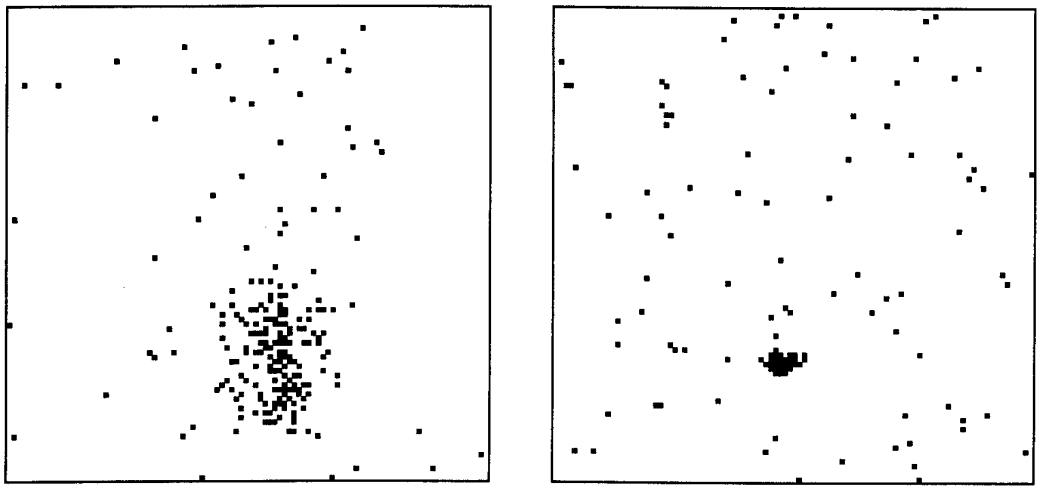

(a) Stage B peak detector *(b) Modified peak detector*

Figure 17 Peak scatter around injected calibration signal

There is an obvious improvement in the consistency of the interpolated position. Also the peaks from noise are more uniformly distributed.

As a measure of the accuracy of the positioning process, the variances of the above scatter plots were determined. This was done by collecting the peak from each dwell with the highest SNR and calculating the sample variance of the time history of these peaks. The sample variance is calculated as follows:

$$\text{var} = \frac{1}{N-1}\sum_{i=1}^{N}\left(x_i - \bar{\mu}\right)^2$$

where $\bar{\mu} = \frac{1}{N}\sum_{i=1}^{N} x_i$ is the sample mean.

Table 7 shows the sample mean and variance of the calibration returns calculated as above. The measurements are in units of cells and cells squared respectively.

		Stage B Algorithm	Modified Algorithm
Range:	Mean	2.52	2.51
	Variance	8.2×10^{-3}	9.6×10^{-5}
Azimuth:	Mean	1.90	1.82
	Variance	4.2×10^{-3}	2.3×10^{-4}
Doppler:	Mean	64.87	64.95
	Variance	2.1×10^{-2}	3.4×10^{-4}

Table 7 Calibration signal location

The position variance has been reduced by a factor of 85 in range and by a factor of 18 in azimuth. This corresponds to factors of more than 9 and 4 respectively in units of standard deviation. This is clearly a very large improvement in position consistency.

7.2 Interpolation Bias

Next we consider the bias of each of the algorithms. For this purpose, we use the same data set. There is a single target, but it does not cause any noticeable impact on the results. Again, all of the peaks were collated for the 188 dwells and then they were plotted in range-azimuth space. A scatter plot of the Stage B peak detector is shown in Figure 18 (a) and the modified detector in Figure 18 (b).

It is apparent from Figure 18 that the new algorithm shows no significant biasing in peak interpolation. In contrast, the previous method shows a considerable degree of clustering of peaks about the cell points. This figure demonstrates the visual impact of the reduction in interpolation bias from all the enhancements that were discussed in this paper. Most of the bias reduction is from data compression and amplitude interpolation. Figure 18 gives a visual interpretation of the histogram variance results expressed in Table 6.

7.3 Tracking

The ultimate improvement in performance should be observed at the tracker output. However, the new peak detector with the adaptive threshold, integrated clutter map and modified data structures cannot be integrated with the Stage B Tracking system. Effort to measure the enhanced peak detector's performance improvement on tracking is not considered worthwhile. Instead, the new peak detector has been

integrated with the Multiple Model Tracker [2]. A test of the fully integrated signal processing and tracking algorithms has been carried out but will not be discussed in this document.

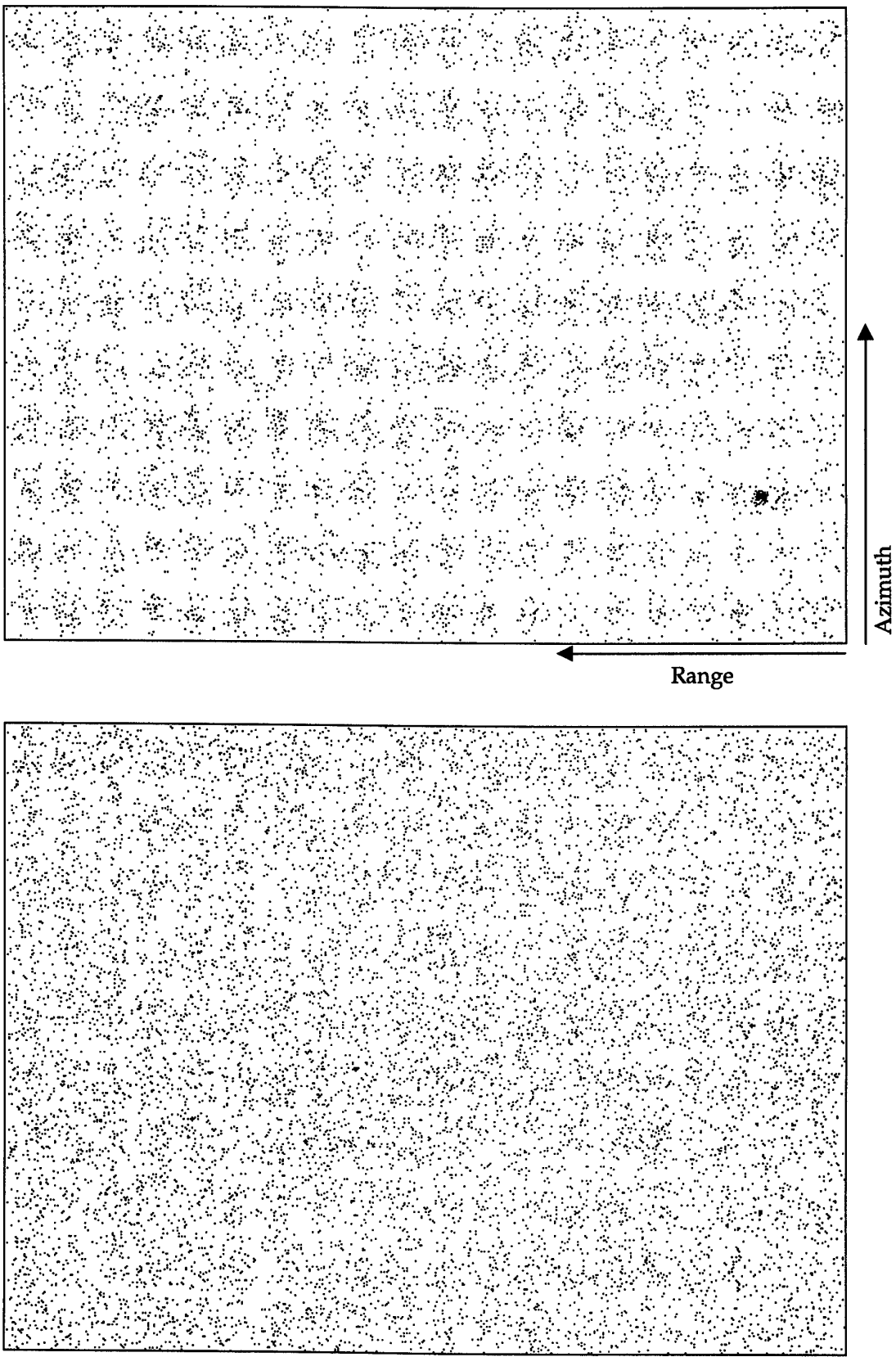

Figure 18 Comparison of peak bias: (a) Stage B system, (b) New system

8. Conclusion

A new algorithm for detection of peaks in 1RSU data has been developed. The new algorithm has been shown to exhibit no significant bias in peak position location and the peak location variance has been dramatically improved. The algorithm has been developed with new data storage structures to enable more flexible detection schemes and non-uniform peak density. The peak detection threshold has been made adaptive to cope with changing clutter conditions.

The new algorithm incorporates the following enhancements:

- Peak interpolation for data in dB in range, azimuth, and doppler for reduced peak bias
- Increased peak detection neighbourhood for reduced peak splitting
- Peak location and interpolation using pre-whitening data for improved position accuracy and reduced peak splitting
- A dynamic peak threshold for adaption to varying clutter conditions
- Flexible data structures that support this adaption

The algorithm has also been incorporated with an adaptive clutter modeling algorithm and integrated with the multiple model track initiation filter. Together with these algorithms it provides an advanced system for target detection and tracking.

References

1. Cox J A
"Evaluation of peak location algorithms with subpixel accuracy for mosaic focal planes", Proc. SPIE Vol. 292 pp. 288-299 1981

2. Colegrove S B
"Advance Jindalee Tracker: PDA Multiple Model Initiation Filter", Defence Science and Technology Organization Technical Report No. DSTO-TR-0659

3. Ristic B and Colegrove S B
"Advanced Jindalee Tracker: Adaptive Clutter Density Model", Defence Science and Technology Organization Technical Report No. DSTO-TR-0804

Appendix A

Linked Lists

The linked list is a simple data structure. Let us consider the problem at a somewhat abstract level. We have some data which we wish to store in an ordered manner. Let us then define the data type node_type as follows:

```
structure {
    data_type       data;
    key_type        key;
    node_type*      next;
    node_type*      previous;
    } node_type;
```

where node_type* denotes a pointer to a record of type node_type using C-like syntax.

This record now contains four elements. Firstly, we have the data that we wish to store. Next we have the key which is used to order the data. Finally, we have two pointers. The idea is that each list entry occupies a separate space in memory. We maintain, at all times, a pointer which points to the first node and by using the pointers stored in each node, we can move forwards or backwards through the list.

This concept is illustrated in Figure 19 below.

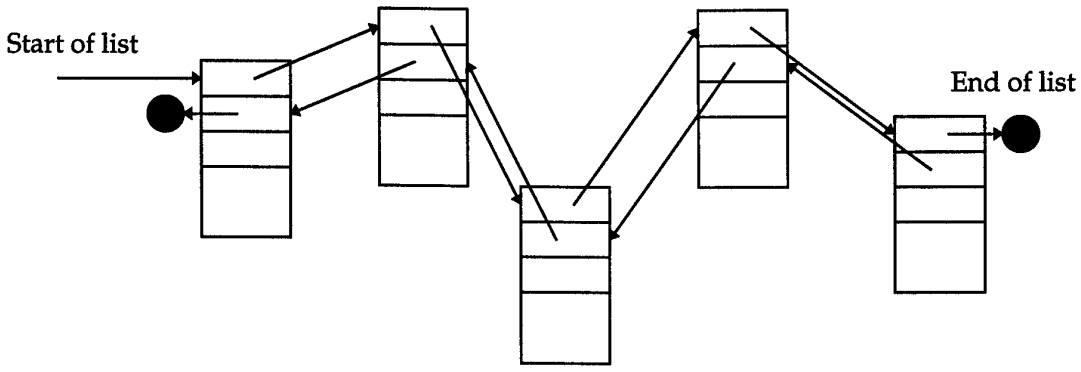

Figure 19 Linked List

It is now a trivial operation to insert a new entry into the list. We simply find the place for it and change the associated pointers. This is in contrast to the use of an ordered array structure, for example, in which we would have to shuffle along the portion of the array after the insertion point to make room.

The same is true also for list entry deletions.

DISTRIBUTION LIST

Advanced Jindalee Tracker: Enhanced Peak Detector

S.J. Davey, S.B. Colegrove & D. Mudge

AUSTRALIA

DEFENCE ORGANISATION

Task Sponsor DGC3ID

S&T Program

Chief Defence Scientist
FAS Science Policy } shared copy
AS Science Corporate Management
Director General Science Policy Development
Counsellor Defence Science, London (Doc Data Sheet)
Counsellor Defence Science, Washington (Doc Data Sheet)
Scientific Adviser to MRDC Thailand (Doc Data Sheet)
Scientific Adviser Policy and Command
Navy Scientific Adviser (Doc Data Sheet and distribution list only)

Scientific Adviser - Army (Doc Data Sheet and distribution list only)

Air Force Scientific Adviser
Director Trials

Aeronautical and Maritime Research Laboratory
Director

Electronics and Surveillance Research Laboratory
Director (Doc Data Sheet and distribution list only)

Chief of Surveillance Systems Division
Research Leader Wide Area Surveillance
Head Tracking and Sensor Fusion
Head Radar Signal Processing
Head Surveillance Systems Integration
Head Electromagnetics and Propagation
Dr S.B. Colegrove
S.J. Davey

DSTO Library
Library Fishermens Bend
Library Maribyrnong
Library Salisbury (2 copies)
Australian Archives
Library, MOD, Pyrmont (Doc Data Sheet only)
Library, MOD, HMAS Stirling
*US Defence Technical Information Center (2 copies)

*UK Defence Research Information Centre (2 copies)
*Canada Defence Scientific Information Service
*NZ Defence Information Centre
National Library of Australia

Capability Development Division
Director General Maritime Development (Doc Data Sheet only)
Director General Land Development (Doc Data Sheet only)
Director General C3I Development (Doc Data Sheet only)
Director General Aerospace Development (Doc Data Sheet only)

Navy
SO (Science), Director of Naval Warfare, Maritime Headquarters Annex,
Garden Island, NSW 2000. (Doc Data Sheet only)

Army
ABCA Office, G-1-34, Russell Offices, Canberra (4 copies)
SO (Science), DJFHQ(L), MILPO Enoggera, Queensland 4051
(Doc Data Sheet only)
NAPOC QWG Engineer NBCD c/- DENGRS-A, HQ Engineer Centre Liverpool
Military Area, NSW 2174 (Doc Data Sheet only)

Air Force

Intelligence Program
DGSTA Defence Intelligence Organisation

Acquisitions Program

Corporate Support Program
OIC TRS, Defence Regional Library, Canberra

UNIVERSITIES AND COLLEGES

Australian Defence Force Academy
Library
Head of Aerospace and Mechanical Engineering
Serials Section (M list), Deakin University Library, Geelong, 3217
Senior Librarian, Hargrave Library, Monash University
Librarian, Flinders University

OTHER ORGANISATIONS

NASA (Canberra)
AGPS
State Library of South Australia ESRL
Parliamentary Library, South Australia

OUTSIDE AUSTRALIA

ABSTRACTING AND INFORMATION ORGANISATIONS

Library, Chemical Abstracts Reference Service
Engineering Societies Library, US
Materials Information, Cambridge Scientific Abstracts, US
Documents Librarian, The Center for Research Libraries, US

INFORMATION EXCHANGE AGREEMENT PARTNERS

Acquisitions Unit, Science Reference and Information Service, UK
Library - Exchange Desk, National Institute of Standards and Technology, US
National Aerospace Laboratory, Japan
National Aerospace Laboratory, Netherlands

SPARES (5 copies)

Total number of copies: 56

DEFENCE SCIENCE AND TECHNOLOGY ORGANISATION
DOCUMENT CONTROL DATA

1. PRIVACY MARKING/CAVEAT (OF DOCUMENT)

2. TITLE

Advanced Jindalee Tracker: Enhanced Peak Detector

3. SECURITY CLASSIFICATION (FOR UNCLASSIFIED REPORTS THAT ARE LIMITED RELEASE USE (L) NEXT TO DOCUMENT CLASSIFICATION)

Document (U)
Title (U)
Abstract (U)

4. AUTHOR(S)

S J Davey
S B Colegrove
D Mudge

5. CORPORATE AUTHOR

Electronics and Surveillance Research Laboratory
PO Box 1500
Salisbury SA 5108 Australia

6a. DSTO NUMBER	6b. AR NUMBER	6c. TYPE OF REPORT	7. DOCUMENT DATE
DSTO-TR-0765	AR-010-822	Technical Report	June 1999

8. FILE NUMBER	9. TASK NUMBER	10. TASK SPONSOR	11. NO. OF PAGES	12. NO. OF REFERENCES
B9505/17/12	ADF 97/004	DGC3ID	31	3

13. DOWNGRADING/DELIMITING INSTRUCTIONS

14. RELEASE AUTHORITY

Chief, Surveillance Systems Division

15. SECONDARY RELEASE STATEMENT OF THIS DOCUMENT

Approved for public release

OVERSEAS ENQUIRIES OUTSIDE STATED LIMITATIONS SHOULD BE REFERRED THROUGH DOCUMENT EXCHANGE, PO BOX 1500, SALISBURY, SA 5108

16. DELIBERATE ANNOUNCEMENT

No Limitations

17. CASUAL ANNOUNCEMENT Yes

18. DEFTEST DESCRIPTORS

Jindalee Stage B Project Peak detection Over the horizon radar

19. ABSTRACT

This paper presents an analysis of the Jindalee Stage B Peak Detector and highlights a number of deficiencies. Solutions are proposed for these deficiencies and the improvements gained from their implementation are measured. These solutions overcome clustering about the data sample points. In addition, enhancements are made in the areas of: adaptive thresholding to maintain a constant false alarm rate, improved data storage to accommodate non-uniform peak densities, and integration with the adaptive clutter model to associate peaks with the clutter regions.